

# Metabolic profiling of a potential antifungal drug, 3-(4-bromophenyl)-5-acetoxymethyl-2,5-dihydrofuran-2-one, in mouse urine using high-performance liquid chromatography with UV photodiode-array and mass spectrometric detection

Milan Nobilis<sup>a,\*</sup>, Milan Pour<sup>b,\*\*</sup>, Petr Šenel<sup>b</sup>, Jan Pavlík<sup>b</sup>, Jiří Kuneš<sup>b</sup>,  
Marie Vopršalová<sup>c</sup>, Lenka Kolářová<sup>d</sup>, Michal Holčápek<sup>d</sup>

<sup>a</sup> Institute of Experimental Biopharmaceutics, Joint Research Center of PRO.MED.CS Praha a.s. and Academy of Sciences of the Czech Republic, Heyrovského 1207, CZ-500 02 Hradec Králové, Czech Republic

<sup>b</sup> Centre for New Antivirals and Antineoplastics, Charles University, Faculty of Pharmacy, Department of Organic and Inorganic Chemistry, Heyrovského 1203, CZ-500 05 Hradec Králové, Czech Republic

<sup>c</sup> Charles University, Faculty of Pharmacy, Department of Pharmacology and Toxicology, Heyrovského 1203, CZ-500 01 Hradec Králové, Czech Republic

<sup>d</sup> University of Pardubice, Faculty of Chemical Technology, Department of Analytical Chemistry, nám.Čs. legií 565, CZ-532 10 Pardubice, Czech Republic

Received 4 December 2006; accepted 22 February 2007

Available online 14 March 2007

## Abstract

3-(4-Bromophenyl)-5-acetyloxymethyl-2,5-dihydrofuran-2-one (LNO-18-22) is a representative member of a novel group of potential antifungal drugs, derived from a natural 3,5-disubstituted butenolide, (-)jincrustoporine, as a lead structure. This lipophilic compound is characterized by high *in vitro* antifungal activity and low acute toxicity. For the purpose of *in vivo* studies, a new bioanalytical high-performance liquid chromatographic method with UV photodiode-array and mass spectrometric detection (HPLC-PDA-MS), involving a direct injection of diluted mouse urine was developed and used in the evaluation of the metabolic profiling of this drug candidate. The separation of LNO-18-22 and its *phase I* metabolites was performed in 37 min on a 125 mm × 4 mm chromatographic column with Purospher RP-18e using an acetonitrile–water gradient elution. Scan mode of UV detection (195–380 nm) was employed for the identification of the parent compound and its biotransformation products in the biomatrix. Finally, the identity of LNO-18-22 and its metabolites was confirmed using HPLC-MS analyses of the eluate. These experiments demonstrated the power of a comprehensive analytical approach based on the combination of xenobiochemical methods and the results from tandem HPLC-PDA-MS (chromatographic behaviour, UV and MS spectra of native metabolites *versus* synthetic standards). The chemical structures of five *phase I* LNO-18-22 metabolites and one *phase II* metabolite were elucidated in the mouse urine, with two of these metabolites having very unexpected structures.

© 2007 Elsevier B.V. All rights reserved.

**Keywords:** Incrustoporine derivatives; 3-(4-Bromophenyl)-5-acetyloxymethyl-2,5-dihydrofuran-2-one (LNO-18-22); Metabolites in mouse urine; HPLC with UV PDA, APCI-MS and ESI-MS detection

## 1. Introduction

Derivatives of 3,5-disubstituted butenolides [1–5] with a certain substitution pattern have been identified as a new class of potential anti-*Aspergillus* antifungal agents, characterized with a small molecular size and high lipophilicity. In particular, 3-(halogenated phenyl)-5-acyloxymethyl-2,5-dihydrofuran-2-ones display a broad *in vitro* antifungal activity,

\* Corresponding author for the bioanalytical part. Fax: +420 495 512 719.

\*\* Corresponding author for the synthetic part.

E-mail addresses: [nobilis@uebfi.cas.cz](mailto:nobilis@uebfi.cas.cz) (M. Nobilis), [pour@faf.cuni.cz](mailto:pour@faf.cuni.cz) (M. Pour).

comparable to that of amphotericin B, as well as relatively low acute toxicity [2,4].

However, no biotransformation and/or pharmacokinetic studies have been made on this promising group of potential antifungals. In particular, a study of the disposition of this emerging class of bioactive substances in the host organism (experimental animal) was an important issue to be addressed. Thus, one of the most active derivatives, 3-(4-bromophenyl)-5-acetyloxymethyl-2,5-dihydrofuran-2-one (LNO-18-22), was selected for disposition studies in mice.

The goal of this study was to develop an HPLC method which would enable us to identify *phase I*, and *phase II* metabolites of 3-(4-bromophenyl)-5-acetyloxymethyl-2,5-dihydrofuran-2-one (LNO-18-22). Hence, the detection of LNO-18-22 metabolites in mouse urine following an intraperitoneal administration of the parent compound was performed. The standards of several expected metabolites were synthesized and the identification of individual LNO-18-22 metabolites was based on the comparison of the chromatographic behaviour, UV and MS spectra of the native metabolites found in the urine and those of the synthesized standards.

## 2. Experimental

### 2.1. Chemicals, preparations and materials

LNO-18-22, 3-(4-bromophenyl)-5-acetyloxymethyl-2,5-dihydrofuran-2-one ( $C_{13}H_{11}BrO_4$ , molecular weight MW = 311.13 g/mol); LNO-18-7, 3-(4-bromophenyl)-5-propoxy-methyl-2,5-dihydro-furan-2-one ( $C_{14}H_{13}BrO_4$ , MW = 325.15

g/mol, I.S.); LNO-18, 3-(4-bromophenyl)-5-hydroxymethyl-2,5-dihydrofuran-2-one ( $C_{11}H_9BrO_3$ , MW = 269.1 g/mol); LN-18, 3-(4-bromophenyl)-5-methyl-2,5-dihydrofuran-2-one ( $C_{11}H_9BrO_2$ , MW = 253.1 g/mol); olefin-18, 3-(4-bromophenyl)-5-methylene-2,5-dihydrofuran-2-one ( $C_{11}H_7BrO_2$ , MW = 251.1 g/mol); PSM1, 3-(4-hydroxyphenyl)-5-hydroxymethyl-2,5-dihydrofuran-2-one ( $C_{11}H_{10}O_4$ , MW = 206.19 g/mol); synthetic mixture containing PSM2, 3-(4-hydroxyphenyl)-5-acetoxymethyl-2,5-dihydrofuran-2-one ( $C_{13}H_{12}O_5$ , MW = 248.23 g/mol) and PSM3, 3-(4-acetoxyphenyl)-5-acetoxymethyl-2,5-dihydrofuran-2-one ( $C_{15}H_{14}O_6$ , MW = 290.27 g/mol); see Fig. 1 for the structures) were synthesized in the laboratories of the Centre for New Antivirals and Antineoplastics.

Phenol (reagent grade) and acetic anhydride (both from Sigma–Aldrich, Prague, Czech Republic) were used for the preparation of phenyl acetate, a comparative standard to PSM-compounds (see Section 3.3). Deuterated solvents ( $CDCl_3$  and  $CD_3OD$ , both from ARMAR Chemicals, Döttingen, Germany) were employed in the NMR analyses. Polyethylene glycol 300 and propylene glycol (both from LACHEMA Brno, Czech Republic) were used for the preparation of the LNO-18-22 injection form. Acetic anhydride, boron tribromide, dichloromethane, ethyl acetate, hexane, pyridine, sodium chloride and sodium sulfate anhydrous (p.a., all from Sigma–Aldrich) were used in the syntheses of PSM1, PSM2 and PSM3 derivatives. Acetonitrile, methanol (both HPLC grade, Merck, Darmstadt, Germany), hydrochloric acid (35% water solution of HCl, analytical grade), ultra-high-quality (UHQ) water prepared using Elgastat UHQ PS apparatus (Elga Ltd.,

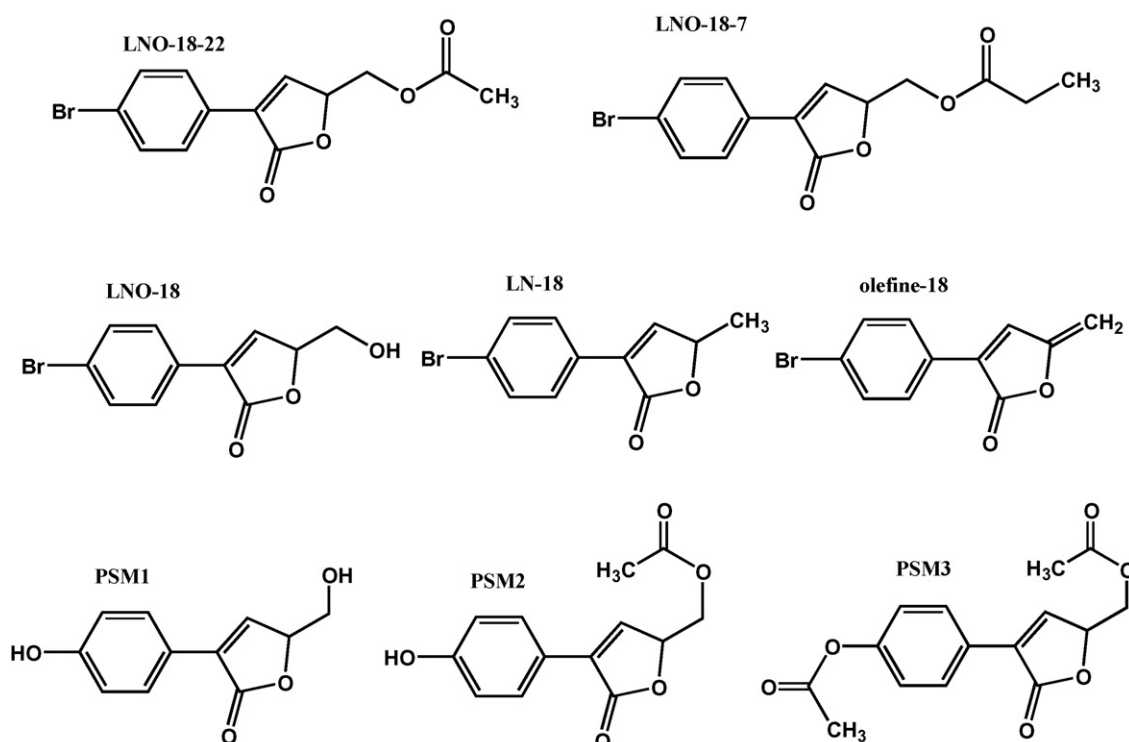


Fig. 1. Chemical structures of the synthetic standards.

Bucks, England) were used in the sample preparation and chromatography of the LNO-18-22 derivatives.  $\beta$ -Glucuronidase (EC 3.2.1.31, type HP-2, 137,800 units/ml), a fluid preparation made from *Helix pomatia* was purchased from Sigma. Acetate buffer (pH 5) was made from 59 ml of 0.2 M acetic acid and 141 ml of 0.2 mol/l sodium acetate.

## 2.2. NMR analyses

A Varian Mercury-Vx BB 300 NMR spectrometer was used for the NMR analyses of the synthetic standards, the derivatives of LNO-18-22. The NMR spectra were recorded at 300 MHz for  $^1\text{H}$ , and 75 MHz for  $^{13}\text{C}$ . Chemical shifts are given as  $\delta$  values in ppm, the coupling constants are given in Hz. Analytical sample (15–20 mg) was dissolved in  $\text{CD}_3\text{OD}$  or  $\text{CDCl}_3$  (0.7 ml) and the solution was transferred *via* pipette into an NMR tube (203 mm length, 5 mm diameter).

## 2.3. HPLC with ultraviolet photodiode-array detection

Routine chromatographic analyses were performed using a Thermo Electron chromatograph. The chromatographic system was composed of an SCM1000 solvent degasser, P4000 quaternary gradient pump, AS 3000 autosampler with a 100  $\mu\text{l}$  sample loop, UV6000LP photodiode-array detector with Light Pipe Technology, SN4000 system controller and data station with the ChromQuest 4 analytical software (Thermo Electron, San Jose, CA, USA).

A LiChroCART 125 mm  $\times$  4 mm chromatographic column containing Purospher RP-18e (5  $\mu\text{m}$ ) with a 4 mm  $\times$  4 mm guard column (the same stationary phase, all from Merck) and a mobile phase containing only acetonitrile and UHQ water in a linear gradient mode were used for the separation of LNO-18-22 and its metabolites. The chromatographic analysis began at the mobile phase composition acetonitrile–UHQ water (20:80, v/v) and a linear gradient increasing gradually the percentage of acetonitrile in the mobile phase to 50% over 20 min was applied. An isocratic mobile phase composition acetonitrile–UHQ water (50:50, v/v) was used in the time interval 20–27 min. A linear gradient gradually decreasing the percentage of acetonitrile in the mobile phase back to 20% in the time interval 27–32 min followed, and the chromatographic analysis was terminated by the equilibration preceding the initial chromatographic conditions: the isocratic elution with acetonitrile–UHQ water (20:80, v/v) in the time interval 32–37 min. The flow rate was 1 ml/min.

A single wavelength mode at 263 nm was used to obtain chromatograms and a photodiode-array mode in the range 195–380 nm with a 1 nm scanning step was applied to record UV spectra of individual compounds. In addition, the identity of LNO-18-22 metabolites in urine was confirmed using HPLC-MS experiments.

## 2.4. HPLC-MS analyses

The chromatographic system was composed of a Model 616 pump with a quaternary gradient system, a Model 996 photodiode-array UV detector, a Model 717+ autosampler,

and a thermostated column compartment (all from Waters, Milford, MA, USA) that was connected to an Esquire 3000 ion trap analyzer (Bruker Daltonics, Bremen, Germany). Atmospheric pressure chemical ionization (APCI) mass spectra were recorded in the mass range  $m/z$  50–800 using both polarity modes and the following setting of the tuning parameters: target mass  $m/z$  = 250, compound stability = 20%, pressure of the nebulizing gas = 70 psi (25 psi for the direct infusion), the drying gas flow rate = 3 l/min, temperatures of the drying gas and APCI heater were 350 and 400  $^\circ\text{C}$  (330 and 350  $^\circ\text{C}$  for the direct infusion), respectively. In many cases, a special setting of the tuning parameters (skimmer 1 = 5 V and capillary exit offset = 130 V) had to be used to suppress an undesired fragmentation of some metabolites. The flow rate of the mobile phase was 1 ml/min (100  $\mu\text{l}/\text{min}$  for the direct infusion) and the injection volume was 100  $\mu\text{l}$ . UV spectra of all chromatographic peaks were recorded in the range 200–400 nm using a photodiode-array UV detector.

The positive- and negative-ion electrospray ionization (ESI) mass spectra of the synthetic standards (LNO-18-22, LNO-18, LNO-18-7 and others) were measured using the direct infusion technique under the following conditions: ion source temperature 300  $^\circ\text{C}$ , the flow rate and the pressure of nitrogen 4 l/min and 10 psi, respectively.

## 2.5. Animals and biological material

Male NMRI mice weighing 29–30 g were used in the experiments approved by the regional ethics committee. Each of a group of six animals received a dose of 200 mg/kg of LNO-18-22 (dissolved in polyethylene glycol 300 and propylene glycol 8:2) intraperitoneally. The animals were placed in glass metabolic cages and urine was collected for 24 h after the administration. All samples were stored at  $-70^\circ\text{C}$  prior to the analysis.

## 2.6. Xenobiochemical experiments and sample preparation of urine to HPLC analysis

Two hundred and fifty microlitre of urine in a tube was mixed with 200  $\mu\text{l}$  of the acetate buffer (pH 5).  $\beta$ -Glucuronidase or just the acetate buffer of pH 5 (16  $\mu\text{l}$ ) was added. The content of the tube was mixed and incubated at 36  $^\circ\text{C}$  for 18 h. The enzymatic reaction was then terminated by the addition of 12.5  $\mu\text{l}$  of concentrated HCl. One hundred microlitres of the incubated mixture were withdrawn and a methanolic solution of LNO-18-7 (15  $\mu\text{l}$  of  $10^{-3}$  mol/l, an internal standard), 105  $\mu\text{l}$  of acetonitrile and 380  $\mu\text{l}$  of UHQ water were added to this sample. After centrifugation (25,000  $\times g$  for 10 min) of the resultant mixture, direct injection of treated and diluted urine samples into the chromatographic column followed.

## 2.7. Physicochemical properties, chromatographic behaviour, NMR and MS analyses concerning the synthesized standards and the metabolites found in urine

The compounds under study were encoded (LNO-18-22, olefin 18, X2, PSM2, etc.), and characterized by molecular weight (MW), retention time ( $t_R$ ) under the chromatographic

conditions described in Section 2.3,  $^1\text{H}$  NMR,  $^{13}\text{C}$  NMR and by MS-data. Short description of the syntheses was also included, when available.

#### 2.7.1. LNO-18-22, MW = 310, $t_R = 21.3$ min [2]

$^1\text{H}$  NMR (300 MHz,  $\text{CDCl}_3$ )  $\delta$  7.76–7.71 (2H, m, AA'BB'), 7.57–7.52 (2H, m overlapped, AA'BB'), 7.53 (1H, d overlapped,  $J = 1.9$  Hz, H4), 5.26–5.21 (1H, m, H5), 4.44–4.32 (2H, m, H6), 2.05 (3H, s,  $-\text{CH}_3$ ).

$^{13}\text{C}$  NMR (75 MHz,  $\text{CDCl}_3$ )  $\delta$  170.60, 170.56, 143.81, 132.16, 131.91, 128.58, 127.84, 124.10, 78.09, 62.84, 20.57.

Negative-ion APCI-MS:  $m/z$  325  $[\text{M}+15]^-$ , 265  $[\text{M}-\text{H}-\text{CO}_2]^-$ , 252  $[\text{M}-\text{CH}_2\text{COO}]^-$ • (100%).

Negative-ion APCI-MS/MS of  $m/z$  325:  $m/z$  283  $[325-\text{CH}_2\text{CO}]^-$ , 265  $[325-\text{CH}_3\text{COOH}]^-$ , 253  $[325-\text{CH}_2\text{CO}-\text{CH}_2\text{O}]^-$ .

Positive-ion APCI-MS:  $m/z$  328  $[\text{M}+\text{NH}_4]^+$ , 311  $[\text{M}+\text{H}]^+$ , 251  $[\text{M}+\text{H}-\text{CH}_3\text{COOH}]^+$  (100%).

Positive-ion APCI-MS/MS of  $m/z$  311:  $m/z$  269  $[\text{M}+\text{H}-\text{CH}_2\text{CO}]^+$ , 251  $[\text{M}+\text{H}-\text{CH}_3\text{COOH}]^+$  (100%), 128  $[\text{M}+\text{H}-\text{CH}_3\text{COOH}-\text{CO}_2-\text{Br}]^-$ •.

Positive-ion APCI-MS/MS of  $m/z$  251:  $m/z$  233  $[\text{M}+\text{H}-\text{CH}_3\text{COOH}-\text{H}_2\text{O}]^+$ , 171  $[\text{M}+\text{H}-\text{CH}_3\text{COOH}-\text{HBr}]^+$  (100%), 128  $[\text{M}+\text{H}-\text{CH}_3\text{COOH}-\text{CO}_2-\text{Br}]^+•$ , 115.

#### 2.7.2. LNO-18-7 (I.S.), MW = 324, $t_R = 24.5$ – $24.9$ min, synthesized according to [2]

$^1\text{H}$  NMR (300 MHz,  $\text{CDCl}_3$ )  $\delta$  7.76–7.70 (2H, m, AA'BB'), 7.58–7.53 (2H, m, AA'BB'), 7.52 (1H, d,  $J = 1.9$  Hz, H4), 5.24 (1H, td,  $J_1 = 1.9$  Hz,  $J_2 = 4.6$  Hz, H5), 4.41 (2H, d,  $J = 4.6$  Hz, H6), 2.33 (2H, q,  $J = 7.6$  Hz,  $-\text{CH}_2-$ ), 1.09 (3H, t,  $J = 7.6$  Hz,  $-\text{CH}_3$ ).

$^{13}\text{C}$  NMR (75 MHz,  $\text{CDCl}_3$ )  $\delta$  174.06, 170.64, 143.84, 132.19, 131.96, 128.60, 127.87, 124.13, 78.24, 62.56, 27.28, 8.98.

Negative-ion APCI-MS:  $m/z$  339  $[\text{M}+15]^-$ , 265  $[\text{M}-\text{H}-\text{CH}_2\text{COO}]^-$ , 252  $[\text{M}-\text{CH}_2\text{CH}_2\text{COO}]^-$ • (100%).

Negative-ion APCI-MS/MS of  $m/z$  339:  $m/z$  283  $[339-\text{CH}_2\text{CH}_2\text{CO}]^-$ , 265  $[339-\text{CH}_3\text{CH}_2\text{COOH}]^-$ , 253  $[339-\text{CH}_2\text{CH}_2\text{CO}-\text{CH}_2\text{O}]^-$ .

Positive-ion APCI-MS:  $m/z$  342  $[\text{M}+\text{NH}_4]^+$ , 325  $[\text{M}+\text{H}]^+$ , 251  $[\text{M}+\text{H}-\text{CH}_3\text{CH}_2\text{COOH}]^+$  (100%), 172  $[\text{M}+\text{H}-\text{CH}_3\text{CH}_2\text{COOH}-\text{Br}]^+•$ , 171  $[\text{M}+\text{H}-\text{CH}_3\text{CH}_2\text{COOH}-\text{HBr}]^+$ , 128  $[\text{M}+\text{H}-\text{CH}_3\text{CH}_2\text{COOH}-\text{CO}_2-\text{Br}]^+•$ .

Positive-ion APCI-MS/MS of  $m/z$  342:  $m/z$  325  $[\text{M}+\text{H}]^+$ , 251  $[\text{M}+\text{H}-\text{CH}_3\text{CH}_2\text{COOH}]^+$  (100%).

Positive-ion APCI-MS/MS of  $m/z$  251: identical as for LNO-18-22.

#### 2.7.3. LNO-18, MW = 268, $t_R = 13.1$ – $13.2$ min [2]

$^1\text{H}$  NMR (300 MHz,  $\text{CDCl}_3$ )  $\delta$  7.76–7.71 (2H, m, AA'BB'), 7.58 (1H, d,  $J = 1.9$  Hz, H4), 7.57–7.52 (2H, m, AA'BB'), 5.15 (1H, ddd,  $J_1 = 1.9$  Hz,  $J_2 = 3.8$  Hz,  $J_3 = 5.2$  Hz, H5), 4.08–3.99 (1H, m, H6a), 3.89–3.80 (1H, m, H6b).

$^{13}\text{C}$  NMR (75 MHz,  $\text{CDCl}_3$ )  $\delta$  171.29, 144.99, 132.08, 131.89, 128.58, 128.06, 123.93, 81.19, 62.77.

Negative-ion APCI-MS:  $m/z$  267  $[\text{M}-\text{H}]^-$ , 239  $[\text{M}-\text{H}-\text{CO}]^-$ , 207  $[\text{M}-\text{H}-\text{CO}-\text{CH}_3\text{OH}]^-$  (100%), 179.

Negative-ion APCI-MS/MS of  $m/z$  267:  $m/z$  249  $[\text{M}-\text{H}-\text{H}_2\text{O}]^-$ , 223  $[\text{M}-\text{H}-\text{CO}_2]^-$ , 205  $[\text{M}-\text{H}-\text{H}_2\text{O}-\text{CO}_2]^-$  (100%).

Positive-ion APCI-MS:  $m/z$  269  $[\text{M}+\text{H}]^+$ , 251  $[\text{M}+\text{H}-\text{H}_2\text{O}]^+$ , 223  $[\text{M}+\text{H}-\text{H}_2\text{O}-\text{CO}]^+$ , 172  $[\text{M}+\text{H}-\text{H}_2\text{O}-\text{Br}]^+•$ , 171  $[\text{M}+\text{H}-\text{H}_2\text{O}-\text{HBr}]^+$ , 128  $[\text{M}+\text{H}-\text{H}_2\text{O}-\text{CO}_2-\text{Br}]^+•$  (100%).

Positive-ion APCI-MS/MS of  $m/z$  269:  $m/z$  251  $[\text{M}+\text{H}-\text{H}_2\text{O}]^+$ , 233  $[\text{M}+\text{H}-2\text{H}_2\text{O}]^+$ , 172  $[\text{M}+\text{H}-\text{H}_2\text{O}-\text{Br}]^+•$ , 128  $[\text{M}+\text{H}-\text{H}_2\text{O}-\text{CO}_2-\text{Br}]^+•$  (100%).

Positive-ion APCI-MS/MS of  $m/z$  251: identical as for LNO-18-22.

#### 2.7.4. Metabolite XI, MW = 248, $t_R = 17.2$ – $17.5$ min

Negative-ion APCI-MS:  $m/z$  248  $\text{M}^-$ • (100%).

Positive-ion APCI-MS:  $m/z$  249  $[\text{M}+\text{H}]^+$  (100%).

#### 2.7.5. Metabolite X2, MW = 266, $t_R = 18.7$ – $18.9$ min

Negative-ion APCI-MS:  $m/z$  265  $[\text{M}-\text{H}]^-$ , 237  $[\text{M}-\text{H}-\text{CO}]^-$ , 209  $[\text{M}-\text{H}-2\text{CO}]^-$  (100%).

Negative-ion APCI-MS/MS of  $m/z$  265:  $m/z$  209  $[\text{M}-\text{H}-2\text{CO}]^-$  (100%), 129  $[\text{M}-\text{H}-2\text{CO}-\text{HBr}]^-$ , 79  $[\text{Br}]^-$ .

Negative-ion APCI-MS/MS of  $m/z$  209:  $m/z$  79  $[\text{Br}]^-$  (100%).

Positive-ion APCI-MS: no signal.

#### 2.7.6. Metabolite X3 = LN-18, MW = 252, $t_R = 22$ – $22.3$ min [1]

$^1\text{H}$  NMR (300 MHz,  $\text{CDCl}_3$ )  $\delta$  7.78–7.71 (2H, m, AA'BB'), 7.56 (1H, d,  $J = 1.9$  Hz, H4), 7.56–7.52 (2H, m, AA'BB'), 5.15 (1H, qd,  $J_1 = 6.8$  Hz,  $J_2 = 1.9$  Hz, H5), 1.52 (3H, d,  $J = 6.8$  Hz,  $-\text{CH}_3$ ).

$^{13}\text{C}$  NMR (75 MHz,  $\text{CDCl}_3$ )  $\delta$  171.10, 149.05, 131.73, 130.29, 128.47, 128.23, 123.57, 76.79, 19.16.

Negative-ion APCI-MS:  $m/z$  251  $[\text{M}-\text{H}]^-$ , 223  $[\text{M}-\text{H}-\text{CO}]^-$  (100%).

Positive-ion APCI-MS: no signal.

#### 2.7.7. Olefin-18, MW = 251, $t_R = 27.1$ – $27.8$ min

LNO-18 (75 mg, 0.28 mmol), triphenylphosphine (88 mg, 0.335 mmol) and imidazole (23 mg, 0.335 mmol) were dissolved in dichloromethane (3 ml), and the solution was stirred at room temperature for 30 min. The solution was then cooled to  $-10$  °C, and a solution of iodine (85 mg, 0.335 mmol) in dichloromethane (3 ml) was added dropwise. The reaction mixture was allowed to warm up to room temperature, diluted with ethyl acetate and washed with saturated aqueous  $\text{Na}_2\text{S}_2\text{O}_3$ . The organic layer was dried over  $\text{Na}_2\text{SO}_4$ , filtered and concentrated *in vacuo*. The product was separated by column chromatography on silica (1:9 ethylacetate/hexanes) to give olefin-18 as a white solid (45 mg, 64%).

$^1\text{H}$  NMR (300 MHz,  $\text{CDCl}_3$ )  $\delta$  7.78–7.71 (2H, m, AA'BB'), 7.56 (1H, d,  $J = 1.9$  Hz, H4), 7.56–7.52 (2H, m, AA'BB'), 5.32 (1H, d,  $J = 2.8$  Hz,  $=\text{CH}_2\text{a}$ ), 5.03 (1H, d,  $J = 2.8$  Hz,  $=\text{CH}_2\text{b}$ ).

### 2.7.8. PSM1, MW = 206, $t_R = 2.8$ min [2]

A solution of  $\text{BBr}_3$  (2 ml, 1 M in  $\text{CH}_2\text{Cl}_2$ , 1.97 mmol) in  $\text{CH}_2\text{Cl}_2$  (2 ml) at  $-50^\circ\text{C}$  was added dropwise to a stirred solution 3-(4-methoxyphenyl)-5-*tert*-butyldimethylsilyloxymethyl-2,5-dihydrofuran-2-one (0.11 g, 0.33 mmol [2]). The mixture was stirred at  $-50^\circ\text{C}$  for 50 min, allowed to warm to room temperature, stirred for another hour and then quenched with water. The mixture was diluted with ethyl acetate and washed with a saturated aqueous sodium chloride. The organic layer was dried with  $\text{Na}_2\text{SO}_4$ , filtered and concentrated *in vacuo*. The crude reaction mixture was purified by column chromatography on silica (6:4 ethylacetate/hexanes) to give PSM1 as white solid (58 mg, 87%).

$^1\text{H}$  NMR (300 MHz,  $\text{CD}_3\text{OD}$ )  $\delta$  7.78–7.71 (2H, m AA', BB', H2', H6'), 7.60 (1H, d,  $J = 1.9$  Hz, H4), 6.84–6.77 (2H, m, AA', BB', H3', H5'), 5.12–5.07 (1H, m, H5), 3.90 (1H, dd,  $J = 12.4$  Hz,  $J = 3.8$  Hz,  $\text{OCH}_2$ ), 3.73 (1H, dd,  $J = 12.4$  Hz,  $J = 4.9$  Hz,  $\text{OCH}_2$ ).

$^{13}\text{C}$  NMR (75 MHz,  $\text{CD}_3\text{OD}$ )  $\delta$  174.4, 159.7, 145.0, 133.0, 129.5, 122.4, 116.3, 83.2, 63.0.

Negative-ion APCI-MS:  $m/z$  205  $[\text{M}-\text{H}]^-$ , 187  $[\text{M}-\text{H}-\text{H}_2\text{O}]^-$  (100%).

Positive-ion APCI-MS:  $m/z$  207  $[\text{M}+\text{H}]^+$ , 189  $[\text{M}+\text{H}-\text{H}_2\text{O}]^+$ , 177  $[\text{M}+\text{H}-\text{CH}_2\text{O}]^+$  (100%).

### 2.7.9. PSM2 + PSM3

Acetanhydride (0.027 ml, 0.28 mmol) was added dropwise to a stirred solution of PSM1 (0.058 g, 0.28 mmol) and pyridine (0.045 ml, 0.56 mmol) in  $\text{CH}_2\text{Cl}_2$  (10 ml) at  $0^\circ\text{C}$ . After all PSM1 was consumed (by TLC), the mixture was concentrated *in vacuo*, diluted with ethyl acetate and washed with a saturated aqueous sodium chloride. The organic layer was dried with  $\text{Na}_2\text{SO}_4$ , filtered and concentrated *in vacuo*. The crude reaction mixture was purified by column chromatography on silica (4:6 ethylacetate/hexanes) to give a mixture of PSM2 and PSM3 as a colourless oil (0.06 g, 85%).

### 2.7.10. PSM2, MW = 248, $t_R = 8.2$ min

$^1\text{H}$  NMR (300 MHz,  $\text{CDCl}_3$ )  $\delta$  7.95–7.85 (2H, m AA', BB', H2', H6'), 7.48 (1H, d,  $J = 1.9$  Hz, H4), 7.20–7.10 (2H, m, AA', BB', H3', H5'), 5.30–5.18 (1H, m, H5), 4.46–4.30 (2H, m,  $\text{OCH}_2$ ), 2.32 (3H, s,  $\text{CH}_3$ ).

Negative-ion APCI-MS:  $m/z$  247  $[\text{M}-\text{H}]^-$ , 187  $[\text{M}-\text{H}-\text{CH}_3\text{COOH}]^-$  (100%), 143  $[\text{M}-\text{H}-\text{CH}_3\text{COOH}-\text{CO}_2]^-$ .

Positive-ion APCI-MS:  $m/z$  266  $[\text{M}+\text{NH}_4]^+$ , 249  $[\text{M}+\text{H}]^+$  (100%), 189  $[\text{M}+\text{H}-\text{CH}_3\text{COOH}]^+$ .

### 2.7.11. PSM3, MW = 290, $t_R = 14$ min

$^1\text{H}$  NMR (300 MHz,  $\text{CDCl}_3$ )  $\delta$  7.82–7.72 (2H, m AA', BB', H2', H6'), 7.38 (1H, d,  $J = 1.9$  Hz, H4), 6.90–6.81 (2H, m, AA', BB', H3', H5'), 5.30–5.18 (1H, m, H5), 4.46–4.30 (2H, m,  $\text{OCH}_2$ ), 2.31 (3H, s,  $\text{CH}_3$ ), 2.06 (3H, s,  $\text{CH}_3$ ).

Negative-ion APCI-MS:  $m/z$  187  $[\text{M}-\text{H}-\text{CH}_3\text{COOH}-\text{CH}_2\text{CO}]^-$  (100%), 143  $[\text{M}-\text{H}-\text{CH}_3\text{COOH}-\text{CH}_2\text{CO}-\text{CO}_2]^-$ .

Positive-ion APCI-MS:  $m/z$  308  $[\text{M}+\text{NH}_4]^+$  (100%), 291  $[\text{M}+\text{H}]^+$ , 231  $[\text{M}+\text{H}-\text{CH}_3\text{COOH}]^+$ , 189  $[\text{M}+\text{H}-\text{CH}_3\text{COOH}-\text{CH}_2\text{CO}]^+$ .

## 3. Results and discussion

As obvious from the structure of LNO-18-22 (see Fig. 1), and based on our experience with the biotransformation of similar compounds, it appeared likely that this molecule could be attacked by hydrolytic enzymes at the most labile ester bond (acyloxymethyl at C5), and the free alcohol LNO-18 would be released through the hydrolysis. It was also expected that LNO-18 would be conjugated to an endogenous substrate (e.g. glucuronic acid), and will be eliminated from the organism in the form of a polar conjugate *via* uropoetic system. This study could therefore help to shed more light on the fate of LNO-18-22 in the organism. In particular, possibility of the metabolic deactivation of these molecules *via* biotransformation processes in the host organism before their actual transport inside the cells of pathogenic fungal guest had to be explored. Similarly, the administered LNO-18-22 might only be a prodrug of an as yet unknown active metabolite. From this point of view, the knowledge of individual chemical structures of all identified LNO-18-22 metabolites would enable their preparation and evaluation of their pharmacological and toxicological properties as well as possible efficiency in antifungal therapy.

### 3.1. Syntheses of the standards and their NMR spectra

LNO-18, LNO-18-22 and LN-18 were prepared according to literature procedures [1,2]; derivative LNO-18-7 was made by the same procedure as LNO-18-22 [2], except that propionyl chloride was used instead of acetyl chloride. Olefin-18 was synthesized from LNO-18 *via* displacement of the OH group with iodine and spontaneous elimination of the *in situ* formed iodomethyl derivative.

Compound PSM1 was formed upon simultaneous desmethylation and desilylation of a known compound [2]. A sample of PSM1 was further converted into a mixture of acetyl derivatives PSM2 and PSM3 by standard acetylation. The structures of all compounds were unequivocally corroborated by NMR and MS methods.

### 3.2. The selection of experimental animal model and sample preparation steps

The male NMRI mice were chosen as a suitable experimental model due to their low distribution volume, and hence a low consumption of the parent compound LNO-18-22 during xenobiochemical experiments. The dose of 200 mg/kg was found to be optimal in preliminary toxicological experiments. With LNO-18-22 being a very lipophilic derivative, the best administration route was an intraperitoneal injection of LNO-18-22, which was dissolved in a mixture of polyethylene glycol 300 and propylene glycol solution. The peritoneal cavity contains well-vascularized abdominal organs (mostly intestinum), which enables a fast transfer of LNO-18-22 into the systemic circulation. Following the distribution and biotransformation of this compound in the mouse organism, the majority of its *phase I* and *phase II* metabolites were excreted *via* the uropoetic system. Thus, urine was selected as the principal, well-processable biomatrix contain-

ing LNO-18-22 metabolites, the chemical structures of which were to be elucidated in this study. The urine was collected for 24 h after the administration of LNO-18-22 using a metabolic cage, which separated urine and faeces and minimized the contamination of the urine by faecal ballast components as well as gastrointestinal microflora. All urine samples were stored at  $-70^{\circ}\text{C}$  prior to the analysis to suppress a possible further microbial biotransformation of the xenobiotics.

The chromatographic conditions described in Section 2.3 were developed for an optimal resolution of synthesized LNO-18-22 derivatives (expected *phase I* metabolites). Possible *phase II* metabolites of LNO-18-22 would have had very short retention times and their peaks would have been hidden among the massive ballast peaks at the start of the chromatogram.

In order to obtain some information about the presence of *phase II*, the experiments with  $\beta$ -glucuronidase (EC 3.2.1.31) were carried out (see Section 2.6, Fig. 2). Polar conjugates (*phase II* metabolites) present in the urine (e.g. LNO-18-glucuronide) were hydrolysed to afford glucuronic acid and the corresponding xenobiotic (LNO-18). The compound released *via* enzymatic hydrolysis increased the amount of LNO-18 present in the urine sample as *phase I* metabolite. Comparative HPLC analyses of a urine sample treated with  $\beta$ -glucuronidase and of the same enzymatically untreated sample are displayed in Fig. 2C).

### 3.3. High-performance liquid chromatography with photodiode-array detection

All LNO-18-22 derivatives depicted in Fig. 1 are practically neutral compounds. Therefore, a simple mobile phase based on acetonitrile–UHQ–water mixture in the gradient mode described in Section 2.3 could be employed for their chromatographic separation. Purospher RP-18e provided the best resolution among tested column packing materials, individual LNO-18-22 derivatives were separated in narrow and symmetric concentration zones (see Fig. 2A). A higher homologue of LNO-18-22 (LNO-18-7) was chosen as an internal standard. The whole analysis of the eight available synthetic standards (including I.S.) lasted 32 min, and each analysis was terminated by a 5 min equilibration interval prior to the establishment of the starting chromatographic conditions.

Chromatograms of the diluted mouse urine having been collected for 24 h after the administration of LNO-18-22 in comparison with the diluted blank mouse urine are shown in Fig. 2B. The parent compound LNO-18-22 was not found in the urine samples, having been completely hydrolyzed to the principal metabolite LNO-18 and/or transformed to some other metabolites (X1, X2, X3, olefin-18), the peaks of which were apparent in the chromatogram (Fig. 2B). As all analyses were done using a UV photodiode-array detector, the UV spectra (and the retention times) of each compound detected in the urine could be immediately studied and compared with synthetic standards. We found that all compounds corresponding to peaks with the retention between  $t_{\text{R}} = 13$  min and  $t_{\text{R}} = 25$  min (Fig. 2B) had the same UV spectrum as the parent LNO-18-22 (see Fig. 3A and B). Thus, the chromophore involving the 3-(4-bromophenyl)-2,5-

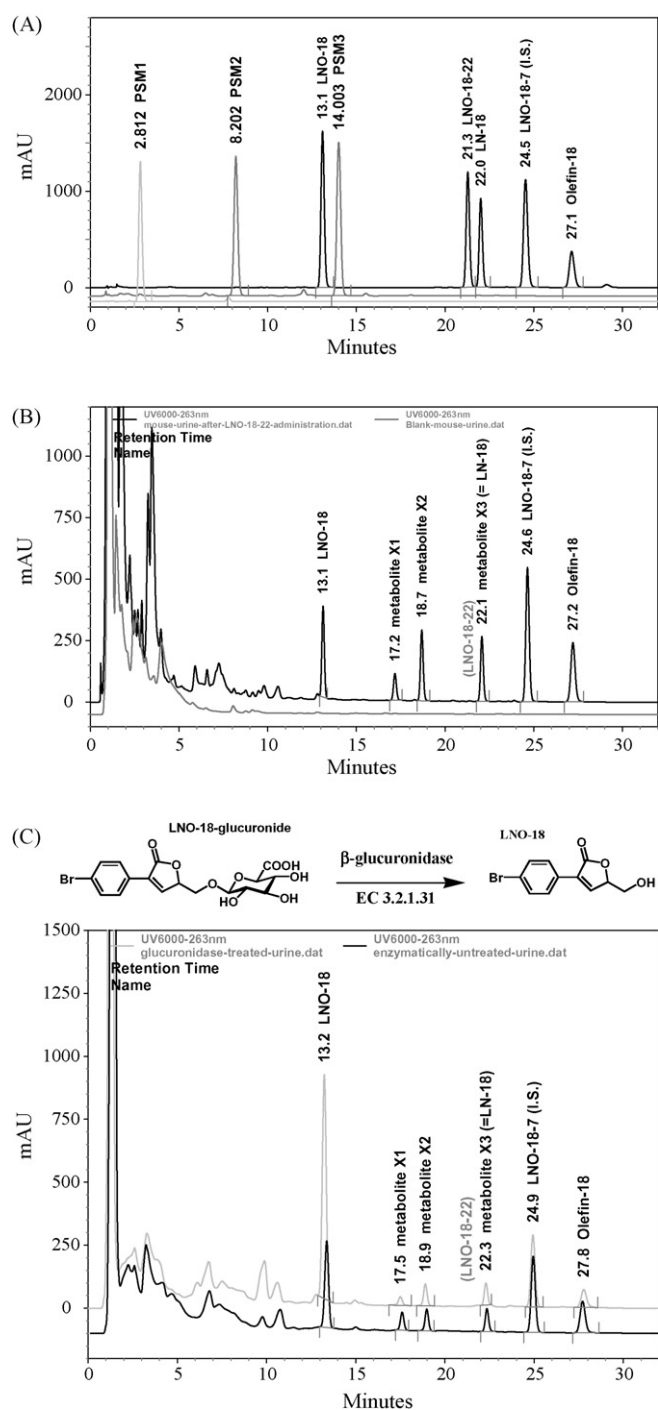


Fig. 2. (A) Chromatographic separation of available standards of LNO-18-22 derivatives (chromatographic conditions described in Section 2.3) demonstrated in three individual chromatograms (grey chromatograms of PSM1 and a synthetic mixture of PSM2 + PSM3 and black chromatogram containing LNO-18 derivatives, LN-18 and olefin-18). (B) Chromatograms of diluted mouse urine after the administration of LNO-18-22 (black line) and diluted blank mouse urine (grey line). (C) Xenobiochemical evidence of the presence of LNO-18-glucuronide in a mouse urine after the administration of LNO-18-22. Chromatogram of the mouse urine treated by the incubation with  $\beta$ -glucuronidase (grey line) in comparison with that of the same enzymatically untreated urine (black line).

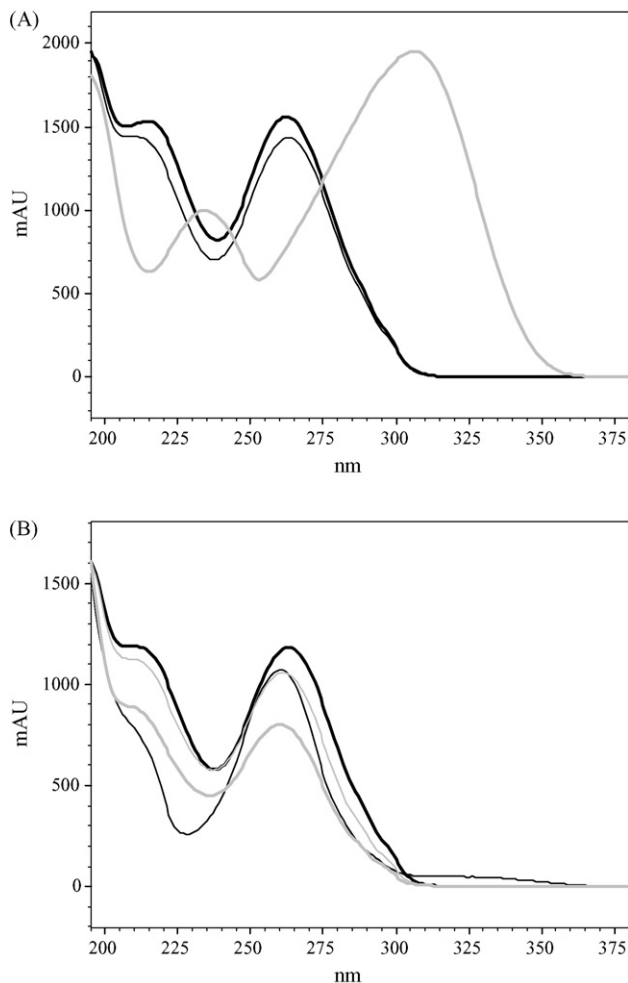


Fig. 3. (A) UV-spectra of compounds LNO-18 (bold black line,  $t_R = 12.8$  min,  $\lambda_{\max} = 213, 263$  nm), LNO-18-22 ( $t_R = 21$  min), LN-18 ( $t_R = 21.7$  min) and LNO-18-7 ( $t_R = 24.2$  min, thin black line,  $\lambda_{\max} = 263$  nm for all three compounds) and olefin-18 (bold grey line,  $t_R = 26.9$  min,  $\lambda_{\max} = 234, 306$  nm). (B) UV-spectra of compounds LNO-18-22 ( $t_R = 21.3$  min, bold black line), metabolites X1 ( $t_R = 17.2$  min, thin black line), X2 ( $t_R = 18.7$  min, bold grey line) and X3 = LN-18 ( $t_R = 22.1$  min, thin grey line);  $\lambda_{\max} = 260\text{--}263$  nm.

dihydrofuran-2-one moiety remained intact in the molecules of the unknown metabolites X1, X2 and X3, and these substances differed probably only in the substitution at C(5).

The synthetic standard LN-18 was found to be identical with the metabolite X3 according to its chromatographic behaviour (retention time), UV spectrum and molecular weight (MW = 252) determined from MS experiments.

The metabolite with the retention time  $t_R = 27.2$  min, identified as olefin-18 (see Fig. 2A and B) displayed a different type of UV spectrum. The methylene group in position 5 is in conjugation with the 3-(4-bromophenyl)-2,5-dihydrofuran-2-one chromophore, and gives rise to a bathochromic shift of the UV spectral maximum from 263 to 306 nm (see the bold grey line of the UV spectrum of olefin-18 in Fig. 3A).

Finally, the chromatographic behaviour, UV and MS spectra of PSM1, PSM2 and PSM3, which were synthesized as the potential LNO-18-22 metabolites, were studied. The chromatographic behaviour is apparent from the chromatograms in

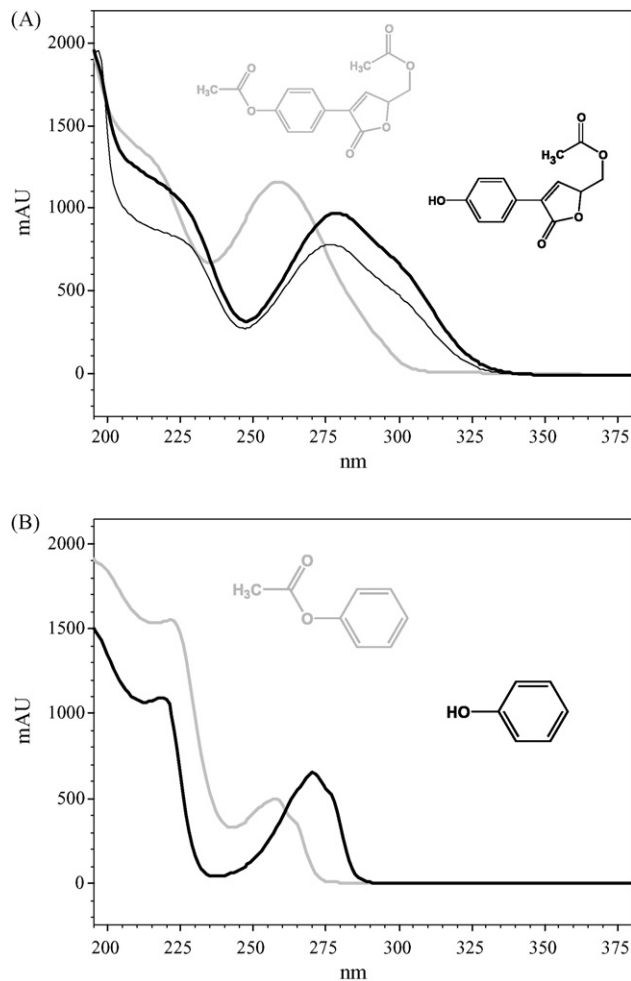


Fig. 4. (A) UV spectra of compounds PSM1 (thin black line,  $t_R = 2.83$  min,  $\lambda_{\max} = 278$  nm), PSM2 (bold black line,  $t_R = 8.22$  min,  $\lambda_{\max} = 278$  nm) and PSM3 (bold grey line,  $t_R = 14$  min,  $\lambda_{\max} = 259$  nm). (B) UV spectra of phenol (black line,  $t_R = 5.53$  min,  $\lambda_{\max} = 218$  nm, 270 nm) and phenyl acetate (grey line,  $t_R = 11.37$  min,  $\lambda_{\max} = 221\text{--}228$  nm, 258 nm) as the simplified chromophore models of PSM2 and PSM3.

Fig. 2A (grey lines). As the lipophilic bromine attached to the phenyl moiety was probably replaced by a hydrophilic hydroxy group, the retention times of PSM1 and PSM2 ranged in the interval of 1–10 min, where the ballast peaks from the urine were eluted (see Fig. 2B). Consequently, the identification of the PSM derivatives would have been complicated. The UV spectra of the PSM derivatives are shown in Fig. 4A. PSM1 was synthesized as a pure compound, while its acetylation led to a mixture of two compounds with the retention times  $t_R = 8.2$  min (PSM2) and  $t_R = 14$  min (PSM3). According to HPLC-MS experiments, PSM2 was identified as the monoacetate of PSM1, while the structure of diacetate was assigned to PSM3. An additional problem arose regarding the position of the acetoxy group in PSM2. PSM1 has both phenolic and alcoholic hydroxy groups in its molecule, and mass spectrometric methods were not able to discriminate between 3-(4-acetoxymethyl)-5-hydroxymethyl-2,5-dihydrofuran-5-one and 3-(4-hydroxymethyl)-5-acetoxymethyl-2,5-dihydrofuran-5-one, since both possible structures of PSM2 have the same molecular weight

(MW = 248). More useful information was provided by UV spectral analysis (see Fig. 4A). As the UV spectra of PSM1 and PSM2 were identical, the same type of chromophore was present in both molecules. Hence, the acetyl moiety in PSM2 must have been bonded to the alcoholic group. Since the acetoxy group is isolated from the chromophore moiety of PSM2 by two  $sp^3$  hybridized carbon atoms, its influence on the PSM2 chromophore is negligible. On the other hand, the acetoxy group attached to the phenolic hydroxyl in PSM3 is in conjugation with the chromophore, and gives rise to a hypsochromic shift of the UV maximum to a shorter wavelength observed in Fig. 4A (grey line).

To confirm the hypsochromic effect, the influence of acetylation on the UV spectra of phenol was studied (see Fig. 4B). Similar to PSM3, the same spectral shift to the shorter wavelength was confirmed in case of phenyl acetate (as a simplified chromophoric model of PSM3, see Fig. 4B).

### 3.4. Mass spectra of the incrustoporine derivatives

Based on the initial comparison of the direct infusion mass spectrometric experiments and HPLC/MS using four ionization modes, i.e., ESI and APCI mass spectrometry both in positive- and negative-ion modes, the APCI has been selected as an optimal ionization technique due to the best sensitivity and information provided for the identification of metabolites. Due to the extensive fragmentation of some metabolites, a special setting of the tuning parameters was necessary to suppress an undesired fragmentation of these metabolites (see Section 2 for more details). The positive-ion APCI mode provided a good ionization efficiency for the standards of studied compounds, LNO-18-22, LNO-18 and LNO-18-7 (I.S.), measured in the direct infusion mode, but the signal-to-noise ratio in the HPLC/MS experiments was so low that the corresponding mass spectra for some unknown metabolites could not be recorded even with an overloaded 100  $\mu$ l injection volume. On the other hand, the negative-ion APCI mass spectra of LNO-18-22 and LNO-18-7 (I.S) suffered from the lack of deprotonated molecules  $[M-H]^-$  and the observed ions  $[M+15]^-$  were quite unusual. The negative-ion APCI mode yielded better results for the metabolites measured in the HPLC/MS run, and the molecular weights (MWs) could be determined on the basis of  $[M-H]^-$  ions for X2 (MW = 266) and X3 (MW = 252) or the molecular radical anion  $M^{\bullet-}$  for X1 (MW = 248). The first-order negative-ion mass spectra of unknown metabolites are shown in Fig. 5. In case of X1, the MW assignment was confirmed by the presence of the  $[M+H]^+$  ion in the positive-ion APCI mass spectrum. The ions  $M^{\bullet-}$  and  $[M+H]^+$  were the only ones observed in the negative- or positive-ion mass spectra of X1, and, consequently, the MW determination was unambiguous. Characteristic isotopic pattern of the bromine atom ( $^{79}\text{Br}$ : $^{81}\text{Br}$  = 1:1) enabled a clear determination of its presence or absence in the individual ions in the mass spectra. The absence of bromine replaced by a free hydroxy group in X1 was easily recognized.

The structures of all three metabolites were proposed on the basis of the data from the first-order mass spectra and tandem

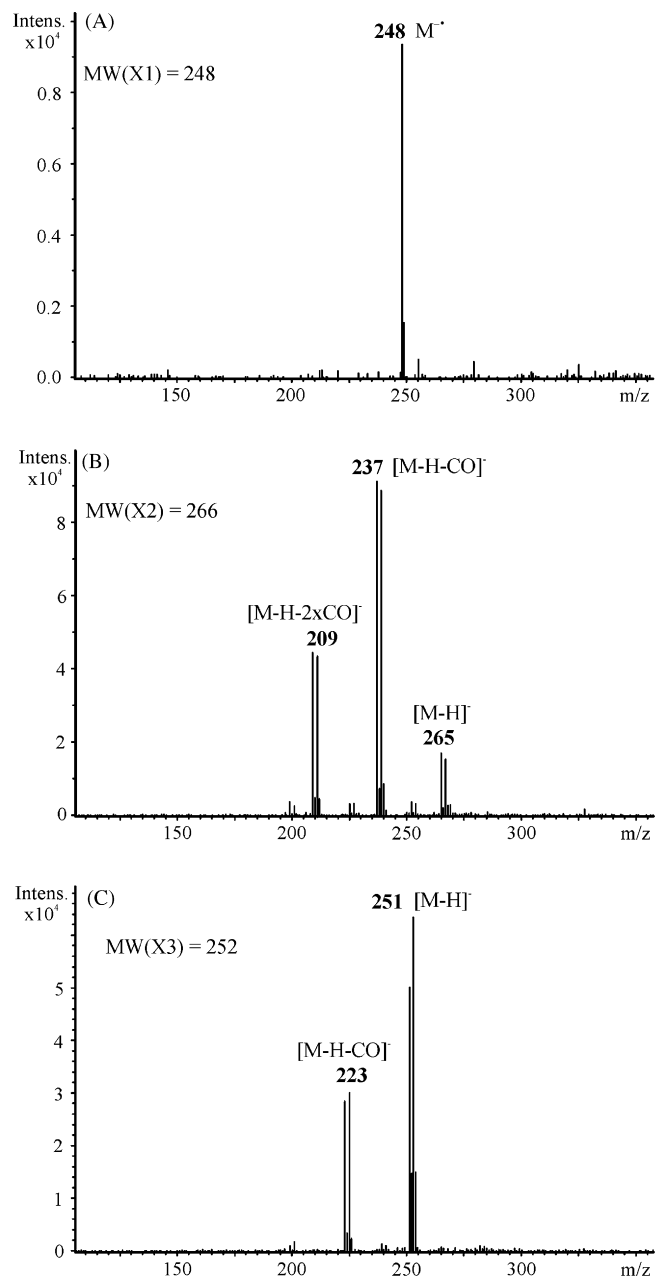


Fig. 5. Negative-ion APCI mass spectra of unknown metabolites: (A) X1 with MW = 248, (B) X2 with MW = 266 and (C) X3 with MW = 252.

mass spectra. To confirm the proposed structures of metabolites X1 and X3, the synthetic standards PSM2 and LN-18, respectively, were used. Both synthetic standards were analyzed under identical conditions as the sample and the spectral data were compared. In case of X3, the chromatographic behaviour, UV and mass spectra were identical to LN-18, and the proposed structure was confirmed. However, the proposed structure of metabolite X1 had to be ruled out, because the chromatographic behaviour of PSM2 was completely different. On the other hand, another metabolite corresponding to PSM2 was additionally found in the sample of the urine. The mass spectra of the new metabolite PSM2 recorded in the positive- and negative-ion mode are shown in Fig. 6.



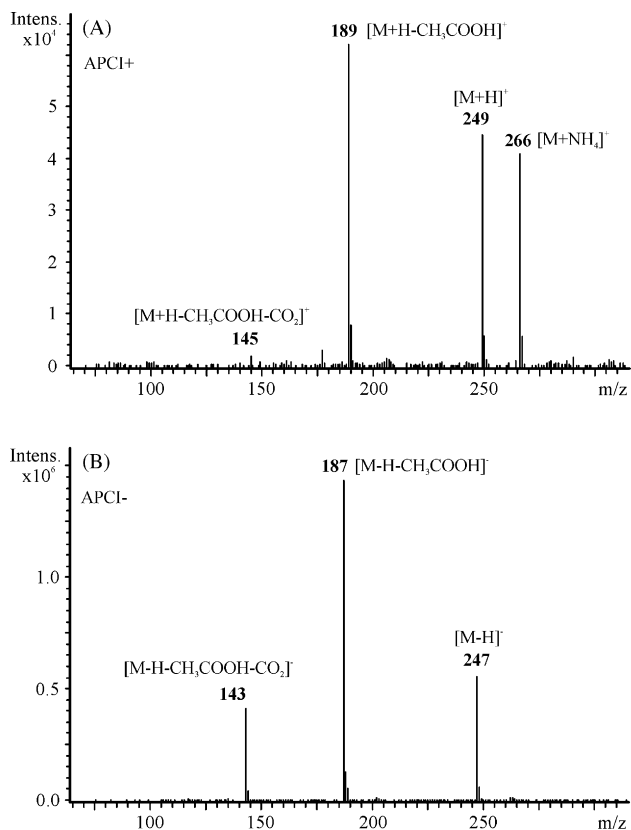


Fig. 6. APCI mass spectra of the new metabolite PSM2 (MW = 248): (A) positive-ion mode and (B) negative-ion mode.

### 3.5. Disposition of LNO-18-22 in mouse

Of the expected *phase I* biotransformation changes in the LNO-18-22 molecule, the hydrolysis of the ester group leading to the alcohol LNO-18 and its consecutive conjugation to an endogenous substrate (glucuronic acid, sulfuric acid or amino acid) to give a polar *phase II* metabolite was very presumptive. Similarly, an oxidation of the alcoholic group of LNO-18 into the corresponding aldehyde and/or finally carboxylic acid could be suggested according to our previous experience. On the other hand, the five-membered unsaturated lactone ring in LNO-18-22 seems to be relatively stable under a range of conditions, and hence a hydrolytic opening of the lactone was not expected. Finally, the bromine atom attached to the phenyl moiety could be replaced by a phenolic hydroxy group *via* arene oxidation or an NIH-shift of bromine into the *meta*-position, and concomitant formation of the *para*-hydroxy group.

The HPLC-DAD-MS experiments confirmed that the labile ester bond in LNO-18-22 was indeed attacked by hydrolytic enzymes, and the free alcohol LNO-18 was released through hydrolysis (see Fig. 2B). This hydrolysis was complete, since no parent compound (LNO-18-22) was found in the chromatograms of the diluted urine of the drug-treated mice.

The presence of the LNO-18-glucuronide in the mouse urine was confirmed by the combination of xenobiochemical and chromatographic experiments (see Fig. 2C and Section 2.6). The mouse urine was divided into two identical portions. The first

portion was treated by  $\beta$ -glucuronidase (see the biotransformation reaction shown in Fig. 2C), while only acetate buffer was added to the second portion. Following the incubation and sample processing described in Section 2.6, the chromatographic analyses of both samples ( $\beta$ -glucuronidase treated urine *versus* enzymatically untreated urine) were compared (see the chromatograms in Fig. 2C). As the peaks of the majority of metabolites and the internal standard were comparable in both analyses, the amount of LNO-18 was significantly (three times) increased in the  $\beta$ -glucuronidase treated urine in comparison with the enzymatically untreated sample. Hence, the polar *phase II* metabolite, LNO-18-glucuronide, was present in the mouse urine, with its peak having been hidden among the ballast peaks at the start of the chromatogram. During enzymatic deconjugation, this *phase II* metabolite was cleaved back into LNO-18, and an increase of the peak of this compound in the  $\beta$ -glucuronidase treated urine was therefore observed.

Very unexpected chemical structures were detected in case of X3 and olefin-18. Even though the quintessence of biotransformation reactions lies in the formation of less lipophilic, less toxic or less irritant compounds and/or more polar metabolites which are well excretable from the organism, both compounds were more lipophilic than the parent LNO-18-22. Olefin-18 was probably formed from LNO-18 or directly from LNO-18-22 *via* an elimination reaction ( $-\text{H}_2\text{O}$  or  $-\text{CH}_3\text{COOH}$ ). The X3 metabolite was found to be identical with LN-18, with its concentration in urine being relatively high. While this compound can, in principle, arise from further biotransformation of olefin-18, the mode of its formation remains unclear.

The possibility of the biotransformation of LNO-18-22 *via* arene oxidation (see Fig. 7) was also considered. 3-(4-Hydroxyphenyl)-5-acetoxymethyl-2,5-dihydrofuran-2-one (PSM2) was identified in low concentration in the urine using the HPLC-MS experiments. The HPLC-PDA was of no use in this case because of the ballast compounds coeluting in the retention time of 8.2 min. Considering the fact that LNO-18-22 was hydrolyzed to LNO-18, it was expected that PSM2 would be hydrolyzed to PSM1. Unfortunately, the standard of this metabolite was eluted in very short retention time (2.8 min), and the native PSM1 metabolite could not be identified by the HPLC-PDA-MS experiments since a massive ballast peak was coeluted in this retention time.

The structure of X2 ( $t_R = 18.9$  min) in the chromatogram in Fig. 2B and C could correspond to the aldehyde, i.e. 3-(4-bromophenyl)-5-formyl-2,5-dihydrofuran-2-one, as this compound had a UV spectrum corresponding to the 3-(4-bromophenyl)-2,5-dihydrofuran-2-one type of chromophore, and the molecular mass derived from the MS-spectra (MW = 266) is in accord with this structure.

The nature of X1 with  $t_R = 17.5$  min in Fig. 2B and C remained unexplained, with no plausible structure being assigned to this substance.

A survey of LNO-18-22 metabolic pathways based on the chemical structures of the metabolites found in the mouse urine is shown in Fig. 7.

Importantly, this xenobiotic study helped to determine future directions in the development of the promising group of poten-

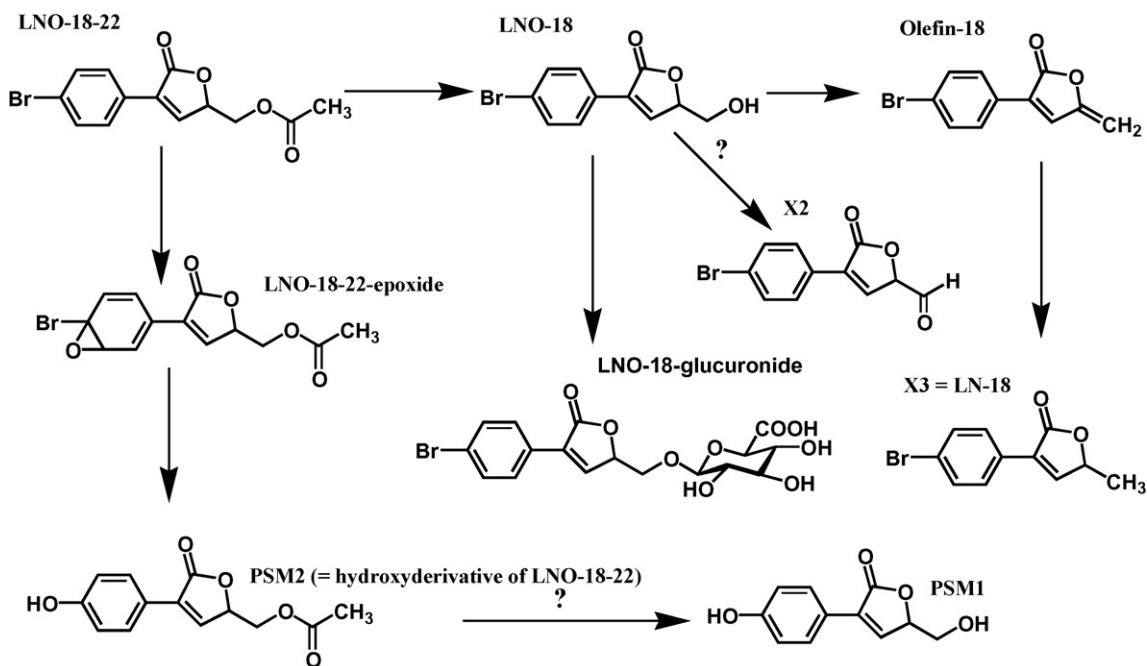


Fig. 7. Survey of the metabolic pathways of LNO-18-22 based on the results of HPLC-PDA and HPLC-MS experiments.

tial antifungal drugs based on the structure of 3-(halogenated phenyl)-5-acyloxymethyl-2,5-dihydrofuran-5-one. LNO-18-22 is easily hydrolysed into the alcohol LNO-18, which was found to be much less active in *in vitro* antifungal essays [2]. Thus, a fast metabolic deactivation of the former in a living organism is likely, and the labile ester bond should therefore be replaced by another one (e.g. amide, a more sterically hindered ester), more stable to the action of esterases. Another possibility to be explored stems from the identification of LN-18. The occurrence of this substance in the urine indicates the possibility of the conversion of LNO-18-22 into olefin-18, which subsequently damages the fungal cell membranes [5] and may be deactivated into LN-18 [1].

In summary, the metabolic pathways of 3-(4-bromophenyl)-5-acyloxymethyl-2,5-dihydrofuran-5-one have been elucidated and major metabolites described. Since the study indicated a high possibility of the fast metabolic deactivation of the drug prototype, structural changes in its molecule are desirable. For this reason, quantitative HPLC determination will be carried out after the labile ester bond is made less prone to enzymatic hydrolysis.

#### 4. Conclusions

A bioanalytical HPLC-PDA-MS method involving the direct injection of enzymatically treated or just diluted mice urine collected after the intraperitoneal administration of the potential antifungal agent LNO-18-22 to experimental animals was developed and employed for the disposition study of this

promising drug in an animal organism. The combination of xenobiochemical methods and the use of hyphenated analytical technique (HPLC-PDA-MS) enabled the elucidation of the chemical structures of principal *phase I* and *phase II* metabolites. In addition, two atypical chemical structures of unusual metabolites were also discovered. The results paved the way for further development and structural modifications of this potential antifungal drug.

#### Acknowledgements

The authors wish to thank to our technician, Mrs. Květa Sládková for her skillful technical assistance. This work was supported by the Ministry of Education of the Czech Republic (Centre for New Antivirals and Antineoplastics 1M0508, projects MSM0021620822 and MSM0021627502) and by the Czech Science Foundation (project No. 203/04/2134).

#### References

- [1] M. Pour, M. Špulák, V. Balšánek, J. Kuneš, V. Buchta, K. Waisser, *Bioorg. Med. Chem. Lett.* 10 (2000) 1893.
- [2] M. Pour, M. Špulák, V. Buchta, P. Kubanová, M. Vopršalová, V. Wsól, H. Fáková, P. Koudelka, H. Pourová, R. Schiller, *J. Med. Chem.* 44 (2001) 2701.
- [3] M. Pour, M. Špulák, V. Balšánek, J. Kuneš, V. Buchta, *Bioorg. Med. Chem.* 11 (2003) 2843.
- [4] V. Buchta, M. Pour, P. Kubanová, L. Silva, I. Votruba, M. Vopršalová, R. Schiller, H. Fáková, M. Špulák, *Antimicrob. Agents Chemother.* 48 (2004) 873.
- [5] L.A. Vale-Silva, V. Buchta, D. Vokurková, M. Pour, *Bioorg. Med. Chem. Lett.* 16 (2006) 2492.